Ion beam synthesis of superconducting MgB_2 thin films

Nianhua Peng[a)]
Advanced Technology Institute, University of Surrey, Guildford, GU2 7XH United Kingdom

G. Shao
School of Engineering (H6), University of Surrey, Guildford, GU2 7XH United Kingdom

C. Jeynes, R. P. Webb, R. M. Gwilliam, and G. Boudreault
University of Surrey Ion Beam Centre, Guildford, GU2 7XH United Kingdom

D. M. Astill and W. Y. Liang
IRC in Superconductivity, University of Cambridge, Cambridge, CB3 0HE United Kingdom

(Received 9 September 2002; accepted 25 November 2002)

Superconducting MgB_2 thin films have been fabricated by 80 keV ^{11}B ion implantation into commercial Mg ribbon with ^{11}B doses up to 10^{18} ions/cm^2, followed by thermal annealing at 500 °C. Temperature dependent dc magnetization measurements confirmed superconducting phase transitions between 11 and 18 K for samples containing nanocrystalline MgB_2 grains embedded in Mg substrate with a small amount of MgO inclusion. © *2003 American Institute of Physics.*
[DOI: 10.1063/1.1537870]

The recent discovery of a superconducting phase transition with $T_c = 39$ K in ceramic MgB_2 has stimulated a wave of world-wide research on superconducting properties of MgB_2 and other related AlB_2 type intermetallic ceramic compounds.[1,2] In addition to impressive progress made for magnet and power applications,[3] promising Josephson junctions have also been fabricated successfully.[4] The simple crystal structure and reasonably high T_c value make MgB_2 a very attractive candidate superconductor for practical applications in the temperature range above 20 K to overcome the low working temperature problem with conventional Nb based superconducting alloys.

Although superconducting MgB_2 powder is available from major chemical suppliers, the preparation of high quality thin film samples is still a technical challenge. So far various thin film preparation methods have been explored in many different laboratories, such as pulsed laser deposition,[5] coevaporation,[6] Mg diffusion,[7] and molecular beam epitaxy growth[8] with various substrates. A serious common problem encountered with MgB_2 thin film fabrication is the high post-deposition annealing temperature employed for producing high T_c superconducting thin films, normally in between 600 and 950 °C. Such a high annealing temperature is not desirable for superconductor device fabrication, as high Mg volatility at temperatures above 600 °C may lead to possible MgB_2 phase decomposition and Mg deficiency in the thin films.[9] In fact, compared to a well defined and reproducible superconducting transition temperature T_c for bulk MgB_2 samples prepared under high pressure with grain size ranging from 0.1 to 10 μm, the reported T_c values for thin film samples vary from one group to another. It is worth noting here that the most important factors influencing the T_c value of polycrystalline thin films might be related to the deposition and annealing conditions but independent of the substrate materials. A low temperature thin film growth approach is of importance for practical applications, particularly an approach with potential for multiple layered Josephson junction fabrication.

Here we describe a MgB_2 thin film preparation approach using 80 keV ^{11}B ion implantation into 99% pure commercial Mg ribbon from Aldrich. The implantation was carried out on a versatile 200 kV Danfysik implanter. During the implantation process the estimate Mg target temperature was about 200 °C with ^{11}B ion beam current about 2 mA. The beam was scanned uniformly over a 200 mm$\times$200 mm area. The total implantation time is about 16 h for an implantation dose up to 10^{18} ions/cm^2. The as implanted samples were followed by various thermal annealing steps at 500 °C either in flowing Ar or vacuum atmosphere. The formation of MgB_2 nanocrystalline phase has been examined by cross-sectional transmission electron microscope (XTEM) and Cu $K\alpha$ x-ray diffraction (XRD) measurements and with depth chemical composition profiles obtained from 1.5 MeV ^4He Rutherford backscattering spectroscopy (RBS). Superconducting phase transitions were observed by temperature dependent dc magnetization measurement using a Quantum Design MPMS superconducting quantum interference device (SQUID) magnetometer with $10^5/4\pi$ A/m dc field applied in parallel to the ribbon plane for temperatures down to 5 K. The typical dimensions of the Mg ribbon used for XRD, RBS, and magnetization measurements are 0.3 mm$\times$3 mm $\times$10 mm. Samples for XTEM observation were prepared by Ar ion milling at room temperature with the ^{11}B implanted Mg ribbon sandwiched by Si wafers.

The elemental depth profiles were extracted from the RBS spectra using Datafurnace code.[10] A multiple scattering correction has been introduced on the Mg signal to ensure a correct subtraction of the background to the ^{11}B signal, using the procedure developed recently by Barradas, Jeynes, and Jackson.[11] To wield Occam's razor effectively during the fitting we link the Mg matrix signal with the low sensitivity signals from the light elements by allowing B and O to be

a)Electronic mail: ees1np@eim.surrey.ac.uk

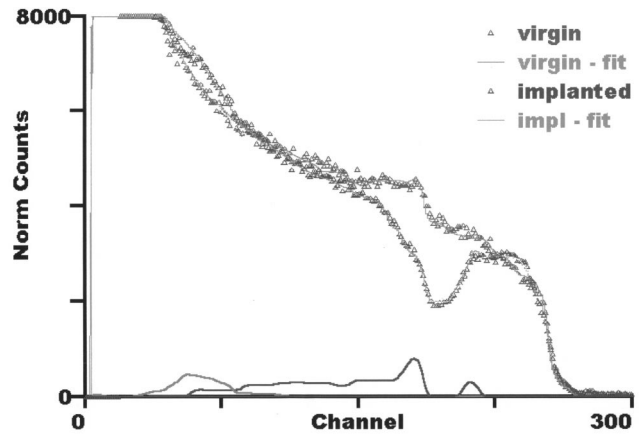

FIG. 1. Observed and fitted RBS data from virgin Mg ribbon and B implanted Mg ribbon.

only in MgB_2 and MgO molecules, respectively.[12] Excellent fitting is obtained showing the validity of the depth elemental profiles obtained, though the raw RBS spectra did not give the chemical information directly.

Figure 1 shows the RBS spectra with the Datafurnace fits for the virgin Mg ribbon and ^{11}B implanted Mg ribbon. The raw RBS data were collected using two detectors simultaneously and the two spectra were fitted together with the Datafurnace. For simplicity of data presentation, only spectra from one detector are shown here. Fitted partial spectra are included only for the annealed sample. All commercial Mg ribbon is oxidized at the surface, but the development of further oxidation following the thermal annealing at 500 °C is dependent on the ^{11}B implantation process. The spectra from the ^{11}B implanted and annealed sample show only slight further oxidation but no significant changes in the ^{11}B profile. In contrast, the spectra from the annealed virgin Mg ribbon show considerable further oxidation after thermal annealing at 500 °C, indicating that the ^{11}B implant acts as a very effective diffusion barrier to oxygen.

The elemental depth profiles obtained for the as implanted sample are shown in Fig. 2. The depth scale is calculated using linear mixtures of the Mg, MgO, and MgB_2 bulk densities (1.73, 3.58, and 2.63 g/cm^3, respectively). There is a region where there is very little free Mg, showing that there is enough B implant to form an almost continuous

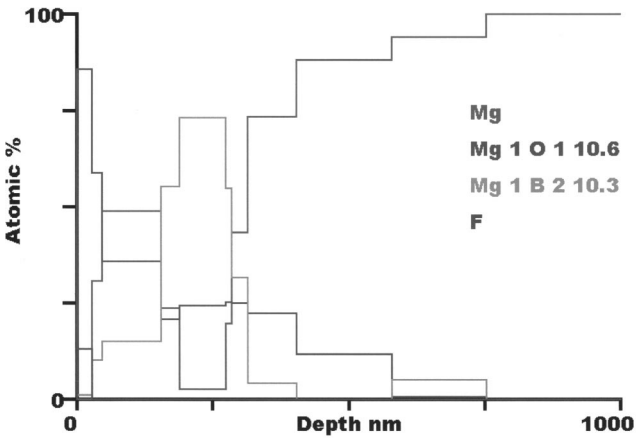

FIG. 2. Elemental depth profiles extracted from RBS for B implanted Mg ribbon.

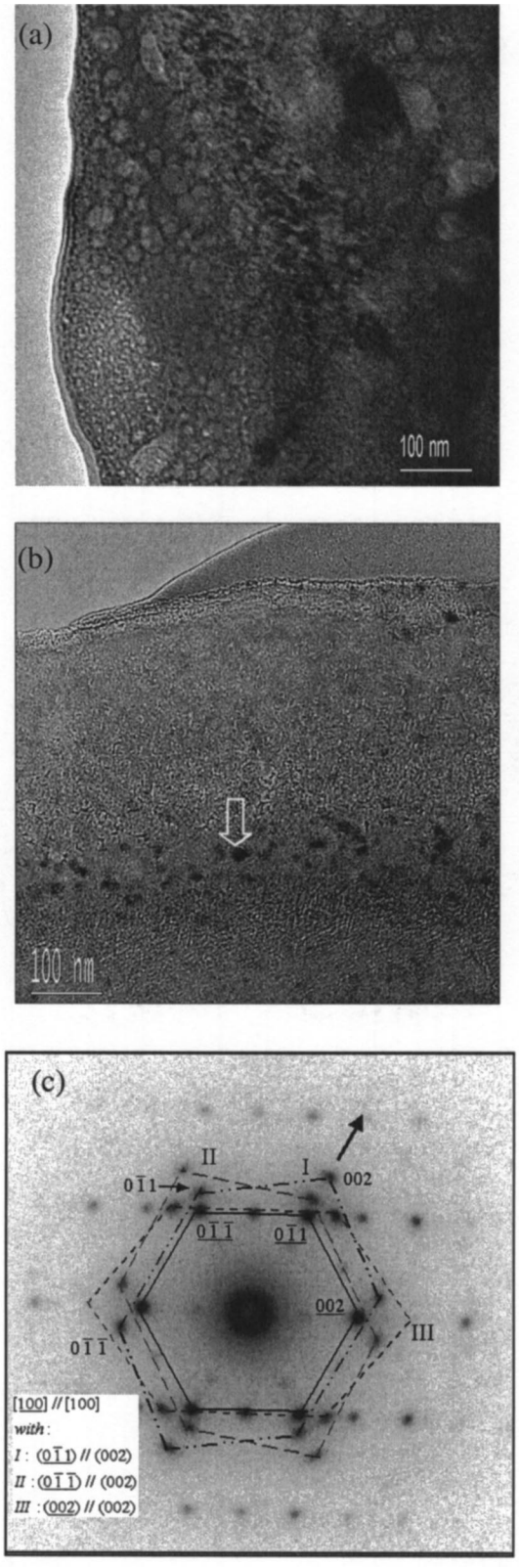

FIG. 3. (a) Bright-field (BF) transmission electron microscopy image of the as implanted sample, showing damage due to the trajectories of implanting ions. (b) BF image of the sample annealed at 500 °C for 15 min, exhibiting nanoscale MgB_2 crystals. (c) Selected area electron diffraction pattern at the $[100]_{Mg}$ zone axis corresponding to (b), where the three orientation variants are indicated, with the indices for the substrate Mg being underlined.

MgB_2 layer. The MgB_2 layer thickness is about 100 nm which is consistent with the simulation using SUSPRE code.[13]

All Cu $K\alpha$ XRD peaks from virgin Mg ribbons and as implanted samples can be easily indexed with a standard Mg

hexagonal structure. Changes in relative diffraction intensities from standard powder diffraction pattern are due to the textures of the ribbons. One prominent effect of ^{11}B ion implantation and following thermal annealing to the Mg target ribbon is the significant change in the preferential texture of the Mg host, due to irradiation damage and regrowth afterwards.

From the available Mg–B binary phase diagram,[9] the most likely phase that could be formed in the Mg/B zone should be MgB_2. Direct evidence for the MgB_2 phase formation has been observed from XTEM. The ^{11}B irradiation damage effect to Mg host is clearly shown in Fig. 3(a). Figure 3(b) shows the sample after thermal annealing at 500 °C for 15 min, nearly all irradiation damaged Mg has been recrystallized and MgB_2 grains are observed, as indicated by the arrow. The maximum dimension of the MgB_2 grain is less than 5 nm. All observable MgB_2 grains are isolated from each other. Figure 3(c) shows the selected area electron diffraction pattern from the MgB_2 grains.

All these experimental facts suggest that Mg/B mixture in the as-implanted sample is more or less still in badly disordered state or even amorphous state. Further growth of MgB_2 grains can be achieved by a thermal annealing step at 500 °C. In fact, weak evidence from XRD for the proper growth of MgB_2 has been observed in a sample annealed at 500 °C for 60 min in flowing Ar atmosphere.

For all as-implanted samples, it is hard to confirm a well defined superconducting phase transition at temperature above 5 K from dc magnetization measurement, though some of them do show very weak transition steps at various temperatures. Annealing at 500 °C for 15 min only, a weak but well defined superconducting phase transition has been observed from the dc magnetization measurement. The 11 K T_c value is considerably lower than the 39 K reported for the bulk material. However, further increase in annealing time at 500 °C improves the T_c value. A much stronger diamagnetic signal has been observed in samples annealed at 500 °C for a longer period, e.g., 30 and 60 min, respectively, as shown in Fig. 4. The XRD patterns for these annealed samples do not show any direct evidence for the formation of MgB_2, an indication of very small grain size of MgB_2 which is beyond the detection limit of the XRD technique.

As all our MgB_2 thin films are embedded inside Mg ribbon with surface layers of MgO, it is worth noting here that special care must be paid to the extraction of the magnetization signal of MgB_2 phase from measured total magnetization data. Pure bulk Mg is a simple paramagnetic metal, however, diamagnetic behavior has been observed in all ^{11}B implanted samples. Such a diamagnetic behavior is even enhanced in those ^{11}B implanted samples following thermal annealing. As the implanted samples had been subjected to a moderate *in situ* beam heating during the implantation process, this diamagnetic behavior might be related to the growth and recrystallization of MgO and formation of nanocrystalline Mg particles, as they can exhibit diamagnetic behaviors at low temperature.[14] Such a diamagnetic contribution to the total magnetization from ^{11}B implanted Mg ribbons might also be the reason for the anomalous high transition temperatures reported in MgB_2 previously.[15]

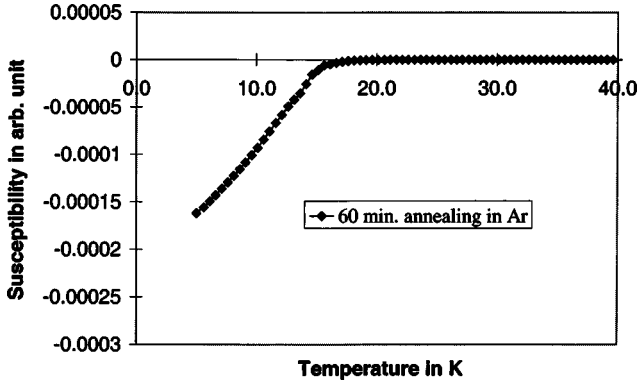

FIG. 4. Temperature dependence of dc susceptibility of a MgB_2/Mg thin films after annealing in flowing Ar for 60 min at 500 °C.

The dependence described earlier of the evolution of the superconducting phase transition temperature T_c value with the annealing condition clearly shows that the suppressed T_c in most of the thin film samples might be related to the small grain size. An extended annealing at low temperature and oxygen free atmosphere seem necessary to grow big and dense MgB_2 grains for high T_c transition. This is consistent with high postdeposition annealing temperature reported before for the formation of high T_c superconducting phase. Actually a recent publication on the low temperature synthesis of superconducting MgB_2 reported a 48 h annealing at 500 °C for a bulk superconducting sample,[16] though the two stage transitions observed there had been explained as weak link behavior associated with the grain boundaries.

[1] J. Nagamatsu, N. Nakagawa, T. Muranaka, Y. Zenitani, and J. Akimitsu, Nature (London) **410**, 63 (2001).
[2] C. Buzea and T. Yamashita, Supercond. Sci. Technol. **14**, R115 (2001).
[3] R. F. Service, Science **295**, 786 (2002).
[4] D. J. Kang, N. H. Peng, R. P. Webb, C. Jeynes, J. H. Yun, S. H. Moon, B. Oh, G. Burnell, E. J. Tarte, D. F. Moore, and M. G. Blamire, Appl. Phys. Lett. **81**, 3600 (2002).
[5] X. H. Zeng, A. Sukiasyan, X. X. Xi, Y. F. Hu, E. Wertz, Q. Li, W. Tian, H. P. Sun, X. Q. Pan, J. Lettieri, D. G. Schlom, C. O. Brubaker, Z. K. Liu, and Q. Li, Appl. Phys. Lett. **79**, 1840 (2001).
[6] W. N. Kang, H. J. Kim, E. M. Choi, C. U. Jung, and S. L. Lee, Science **292**, 1512 (2001).
[7] A. Plecenik, L. Satrapinsky, P. Kus, S. Gazi, S. Benacka, I. Vavra, and I. Kostic, Physica C **363**, 224 (2001).
[8] K. Ueda and M. Naito, Appl. Phys. Lett. **79**, 2046 (2001).
[9] Z. K. Liu, D. G. Schlom, Q. Li, and X. X. Xi, Appl. Phys. Lett. **78**, 3678 (2001).
[10] N. P. Narradas, C. Jeynes, and R. P. Webb, Appl. Phys. Lett. **71**, 291 (1997).
[11] N. P. Narradas, C. Jeynes, and S. M. Jackson, Nucl. Instrum. Methods Phys. Res. B **138**, 1168 (1998).
[12] C. Jeynes, N. P. Narradas, H. Rafla-Yuan, B. P. Hichwa, and R. Close, Surf. Interface Anal. **30**, 237 (2000).
[13] R. P. Webb, in *Practical Surface Analysis*, 2nd ed. edited by D. Briggs and M. Seah (Wiley, Chichester, 1992), Vol. 2, pp. 657–704.
[14] K. Kimura, S. Bandow, and S. Sako, Surf. Sci. **156**, 883 (1985).
[15] M. Majoros, B. A. Glowacki, and M. E. Vickers, Supercond. Sci. Technol. **15**, 269 (2002).
[16] N. Rogado, M. A. Hayward, K. A. Regan, Y. Y. Wang, N. P. Ong, H. W. Zandbergen, J. M. Rowell, and R. J. Cava, J. Appl. Phys. **91**, 274 (2002).